

Ta₃N₅/Polymeric g-C₃N₄ as Hybrid Photoanode for Solar Water Splitting:

Author: Mengdi Liu

Persistent link: <http://hdl.handle.net/2345/bc-ir:108366>

This work is posted on [eScholarship@BC](#),
Boston College University Libraries.

Boston College Electronic Thesis or Dissertation, 2018

Copyright is held by the author, with all rights reserved, unless otherwise noted.

Boston College

The Graduate School of Arts and Science Department of Chemistry

Ta₃N₅/POLYMERIC g-C₃N₄ AS HYBRID PHOTOANODE FOR
SOLAR WATER SPLITTING

A thesis by

MENGDI LIU

Submitted in partial fulfilment of the requirements for the degree of

Master of Science

Nov 2018

Ta₃N₅/Polymeric g-C₃N₄ as Hybrid Photoanode for Solar Water Splitting

Mengdi Liu

Advisor: Prof. Dunwei Wang

Abstract

Water splitting has been recognized as a promising solution to challenges associated with the intermittent nature of solar energy for over four decades. A great deal of research has been done to develop high efficient and cost-effective catalysts for this process. Among which tantalum nitride (Ta₃N₅) has been considered as a promising candidate to serve as a good catalyst for solar water splitting based on its suitable band structure, chemical stability and high theoretical efficiency. However, this semiconductor is suffered from its special self-oxidation problem under photoelectrochemical water splitting conditions. Several key unique properties of graphitic carbon nitride (g-C₃N₄) render it an ideal choice for the protection of Ta₃N₅. In this work, Ta₃N₅/g-C₃N₄ hybrid photoanode was successfully synthesized. After addition of co-catalyst, the solar water splitting performance of this hybrid photoanode was enhanced. And this protection method could also act as a potential general protection strategy for other unstable semiconductors.

Keywords

Ta₃N₅, g-C₃N₄, Water Oxidation, Photoelectrochemistry.

Table of Contents

Chapter 1: Introduction	1
1.1 Tantalum Nitride as Photoanode for PEC Water Splitting	1
1.2 Graphitic Carbon Nitride (g-C ₃ N ₄) as Protection Layer for Ta ₃ N ₅	3
1.3 Research Opportunities	4
Chapter 2: Experiment Section	7
2.1 Preparation of Ta ₃ N ₅ Nanotube (NT) Photoelectrodes	7
2.2 Preparation of Cubic Ta ₃ N ₅ Photoelectrodes	8
2.3 Synthesis of Ta ₃ N ₅ /polymeric g-C ₃ N ₄ Hybrid Photoanode	8
2.4 Deposition of Co-Pi, Co(OH) ₂ , NiFeOOH and CoNiFeOOH co-catalysts.	9
2.5 Deposition of GaN.....	10
2.6 PEC Measurement	10
2.7 Materials Characterization.....	11
Chapter 3: Data Analysis and Discussion	12
3.1 Ta ₃ N ₅ NTs/g-C ₃ N ₄ Hybrid Material as Photoanode.	12
3.1.1 Materials Characterization.....	12
3.1.2 PEC Performance of Ta ₃ N ₅ NTs/g-C ₃ N ₄ Hybrid Material.....	13
3.2 Cubic Ta ₃ N ₅ /g-C ₃ N ₄ Hybrid Material as Photoanode.....	16
3.2.1 Materials Characterization.....	16
3.2.2 PEC Performance of Cubic Ta ₃ N ₅ /g-C ₃ N ₄ Hybrid Material	17
3.3 Ta ₃ N ₅ NTs/GaN as Photoanode.	18
3.3.1 Materials Characterization.....	18
3.3.2 PEC Performance of Ta ₃ N ₅ /GaN Material	20
Chapter 4: Conclusion.....	22
Reference	23

Chapter 1: Introduction

Solar energy is a clean and abundant source of energy available over the entire planet. The capture of solar energy and its conversion to storable chemical fuel by photoelectrochemical (PEC) systems provides a promising route to overcoming the current global reliance on fossil fuels.¹⁻⁴ Since the work done by Fujishima and Honda in 1972, a great deal of research efforts has been inspired to realize this dream that is often referred to as artificial photosynthesis.⁵⁻⁶ However, challenges related to the development of high performance photoanodes have long thwarted the practical applications of water splitting devices. The field has come a long way since the initial demonstration, and exciting progress has been made. In the past decades, the advance of materials science and electrode fabrication technologies has expanded this area greatly. As far as efficiencies are concerned, >12% has been demonstrated by several different systems.⁷⁻⁸ The overall progress, however, has been frustratingly slow. PEC water splitting still faces the problems of low efficiency, poor stability, and high cost. Much effort has been devoted to energy band tuning and morphology control. To date, water splitting as a practical solar energy harvesting technology remains unrealistic. However, since there are no theoretical reasons why the process cannot be both efficient and inexpensive, the slow progress intrigues the scientific community. After all, solar water splitting may be the only technology that can meet our energy demand on the terawatts scale in a solar energy-powered future in the long run.⁹

1.1 Tantalum Nitride as Photoanode for PEC Water Splitting

Suitable energy band positions, absorption of long wavelength light, efficient charge separation and high catalytic activity are important properties for materials to be used for water splitting.¹⁰ Metal nitrides or metal oxy-nitrides offer wider light adsorption spectrum and better band position for solar water splitting, they have been extensively studied among these years.¹¹⁻¹² As an n-type semiconductor, tantalum nitride (Ta_3N_5)

has recently emerged as a promising photoanode material. It features a direct band gap of 2.1 eV with high light absorption coefficients (e.g., it absorbs >60% of photons at $\lambda=500$ nm within a thickness of 100 nm) which offers it the potential to be a good PEC water splitting catalyst.¹³ Moreover, the conduction and valence band edge positions as measured by ultraviolet photoelectron spectroscopy (UPS) and Mott-Schottky plots indicate that they can straddle the water splitting potentials, which predicts theoretical photovoltages >1.23 V.¹⁴ Furthermore, near-theoretical-limit photocurrent density of 12.1 mA/cm² at 1.23 V vs. reversible hydrogen electrode for water oxidation has already been reported, supporting that charge transport is not a limiting factor in defining the performance Ta₃N₅.¹⁵ With all above, it is predicted that a solar-to-hydrogen efficiency exceeding 10% is possible when Ta₃N₅ is coupled with a practical SiNWs photocathode in a tandem solar water splitting configuration (Fig. 1b).

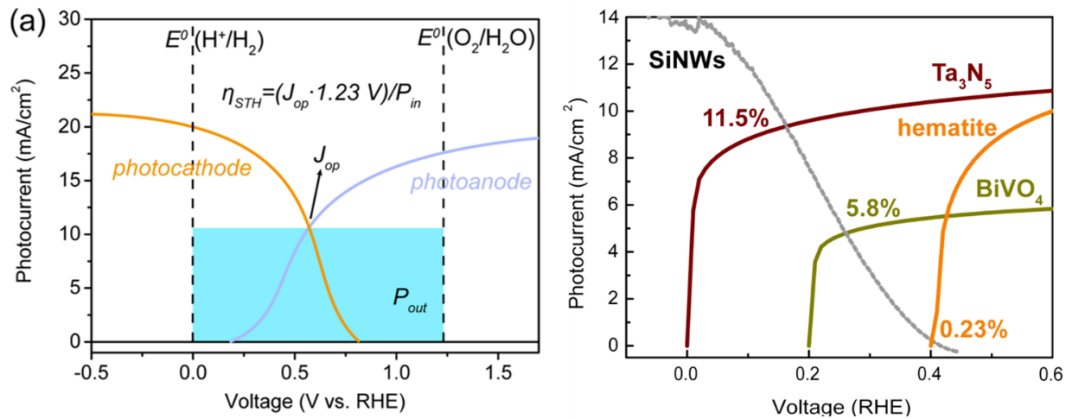


Figure 1. (a) Current-voltage behavior for a photocathode and a photoanode. (b) Theoretical water splitting efficiencies by various photoanode materials when coupled with experimental data of a not yet optimized Si nanowires (SiNWs) photocathode. The J-V curves of photoanodes were calculated based on the Gärtner equation. The SiNWs data were obtained with simulated sunlight (AM 1.5; $\lambda>600$ nm only) in our lab.

However, two remaining critical issues still limit the practical performance of Ta₃N₅. First, the high photovoltage expected from Ta₃N₅ has not been achieved. In fact, in most of cases, more positive than 0.6 V vs. RHE of turn-on potential was obtained. The expected turn-on based on the measured band edge and flatband positions should be

more negative than 0 V. Its poor stability is another issue that needs to be addressed. For instance, the photoactivity of Ta_3N_5 is completely suppressed within several minutes of operations when it was under no protection.¹⁶⁻¹⁷

1.2 Graphitic Carbon Nitride ($\text{g-C}_3\text{N}_4$) as Protection Layer for Ta_3N_5

Several key unique properties of $\text{g-C}_3\text{N}_4$ render it an ideal choice for the protection of Ta_3N_5 . As a two-dimensional (2D) material, $\text{g-C}_3\text{N}_4$ is convenient to prepare. By the decomposition of C- and N-containing precursors at moderate temperatures, it can be easily obtained.¹⁸ Band gap of graphene is highly affected by its thickness while $\text{g-C}_3\text{N}_4$ features a bandgap (~1.9-2.9 eV) regardless of its size.¹⁹ Furthermore, $\text{g-C}_3\text{N}_4$ has been shown to be a stable material that can survive the harsh reaction conditions of water oxidation and reduction.²⁰ The stability of $\text{g-C}_3\text{N}_4$ under oxidizing conditions may appear surprising since the majority of published works on this material focused on studying its reduction properties. That fact that multiple groups have reported the stability under different conditions in the past years strongly support that the stability against oxidation is reproducible.²⁰⁻²¹ For this work, we are particularly attracted to the following features offered by $\text{g-C}_3\text{N}_4$.

First, the 2D nature of $\text{g-C}_3\text{N}_4$ makes it possible to form a thin but uniform coverage on a nanostructured photoelectrode surface. It has been shown, for example, that the nanosheet of $\text{g-C}_3\text{N}_4$ can form a conformal contact with either planar or nanostructured substrates.²² This property opens up the possibility of using $\text{g-C}_3\text{N}_4$ as a protection (or passivation) layer.

Second, $\text{g-C}_3\text{N}_4$ has been shown as an effective water oxidation catalyst (WOC).²³⁻²⁴ For other well-known WOCs such as RuO_2 or NiFeOOH which showed a four electron pathway for water oxidation, $\text{g-C}_3\text{N}_4$ proceeds through a 2-electron pathway to produce H_2O_2 .²⁵⁻²⁷ However the as-form H_2O_2 also has a poisoning effect toward $\text{g-C}_3\text{N}_4$ itself. A recent report offered a nice solution by adding H_2O_2 decomposition catalysts which helped recovering the activity of $\text{g-C}_3\text{N}_4$.²⁸

Third, g-C₃N₄ was a nice WOC which contains no O element. Such a feature is a key reason why we choose it for this study. Our recent study on Ta₃N₅ as a promising photoanode revealed that the surface N content would be easily replaced by O species during water oxidation and this phenomenon further killed the catalysts.¹⁶ It fulfills our goal that Ta₃N₅ will not undergo self-oxidation by removal of O species, and it may possibly be used as general protection method of other non-oxide photoanode materials. g-C₃N₄ provides a unique opportunity to test this hypothesis. With all special properties mentioned above, g-C₃N₄ will potentially act as a dual-function layer for solar water oxidation applications. We plan to apply it to Ta₃N₅ and expect dramatic improvement in terms of turn-on potential and stability.

1.3 Research Opportunities

A great deal research has been focused on Ta₃N₅ due to its The potentiality and challenges. Domen's group applied a series of WOCs like IrO₂ and Co-Pi on Ta₃N₅ to improve its stability. Although their catalyst can survive for over 100 min, the turn-on potential was never improved.²⁹⁻³¹ After this, they recognized the importance of the turn-on potential and employed an Mg and Zr co-doping scheme, together with the application of CoO_x/FeO_x WOCs, but only obtained a modest improvement to 0.55 V.³² To the best of our knowledge, the most important the question that what the true origins for the two critical issues are has not been not been answered by these previous reports. It still a critical issue for the unexpected high turn-on potential for Ta₃N₅.

The true reasons behind the key issues are often poorly understood. Issues surrounding Ta₃N₅ offered a nice example of challenges encountered by most researchers in water splitting field. In recognition of this deficiency, we recently embarked on a detailed study to understand what limits the performance of Ta₃N₅. Using a combination of X-ray absorption spectroscopy (XAS), X-ray photoelectron spectroscopy (XPS, including ambient pressure XPS) and PEC techniques, we discovered that both the high turn-on potential and the poor stability of Ta₃N₅ are due to severe Fermi level pinning as a result of surface N atom displacement by O during

water oxidation. A quantitative correlation between the degree of surface oxidation and the extent of surface Fermi level pinning was established (Fig. 2). The key conclusion we drew from this body of research was that the performance of Ta_3N_5 is limited by a self-limiting surface oxidation process.¹⁶ We are therefore inspired to hypothesize that low V_{on} and good stability can be obtained on Ta_3N_5 by a non-oxide coating. The coating has to be non-oxide because the presence of O is expected to displace the N atoms and induce severe surface Fermi level pinning to compromise the overall performance.

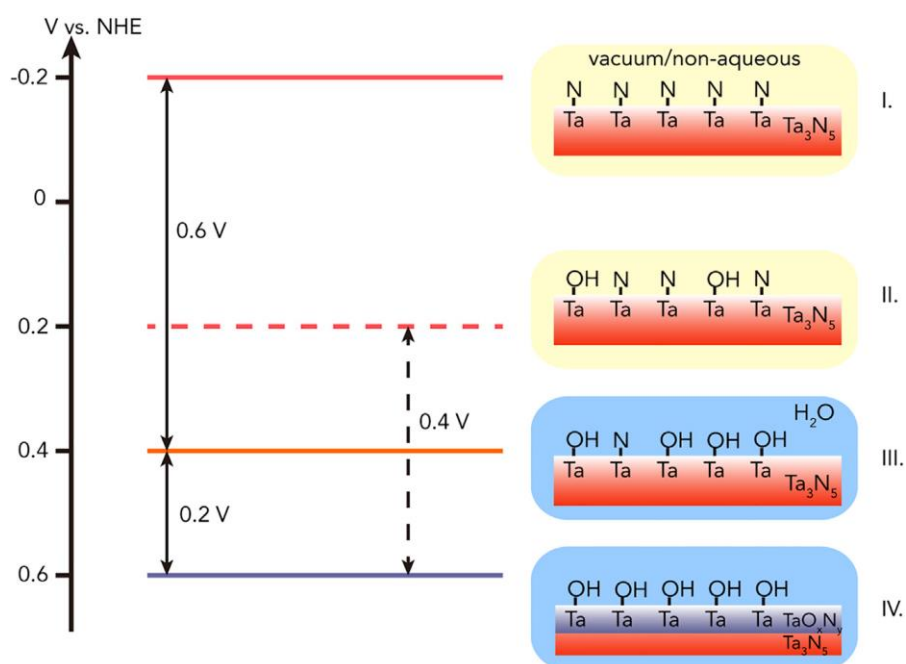


Figure 2. The Evolution of Ta_3N_5 Surface Energetics

Stage I: fresh Ta_3N_5 free of H_2O .

Stage II: Ta_3N_5 with partial H_2O adsorption due to exposure to ambient air.

Stage III: Ta_3N_5 immersed in H_2O .

Stage IV: Ta_3N_5 with surface oxides. The horizontal lines correspond to the surface Fermi-level position of Ta_3N_5 in stages I–IV.

Reproduced from Ref. 13.

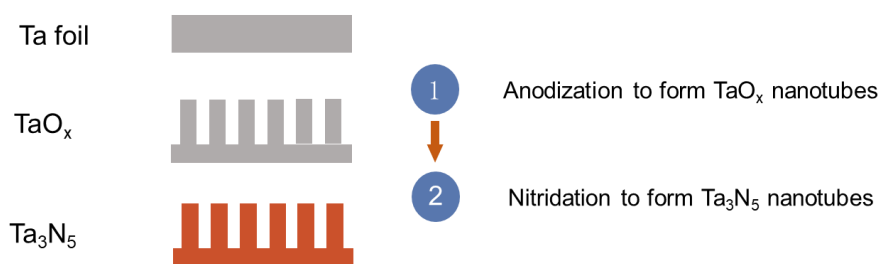
Our hypothesis as stated above presents a unique system that features all desired properties for solar water oxidation. By combining it with existing photocathodes (e.g., Si nanowires, SiNWs), high-efficiency overall solar water splitting becomes possible (Fig. 1b). Testing the hypothesis constitutes the major objective of this proposal. It is

highlighted that the resulting material, $\text{Ta}_3\text{N}_5/\text{g-C}_3\text{N}_4$ is fundamentally different from other high-efficiency solar water splitting systems such as p-n GaAs/GaInP₂ or the Si triple junction in its simplicity and operation principles.^{8,33} While the other systems are all based on buried junction photovoltaic modules, the $\text{Ta}_3\text{N}_5/\text{g-C}_3\text{N}_4$ relies on the photoelectrode/water interface to separate charges. It provides an opportunity to study the fundamental principles of a PEC system.

Chapter 2: Experiment Section

2.1 Preparation of Ta₃N₅ Nanotube (NTs) Photoelectrodes

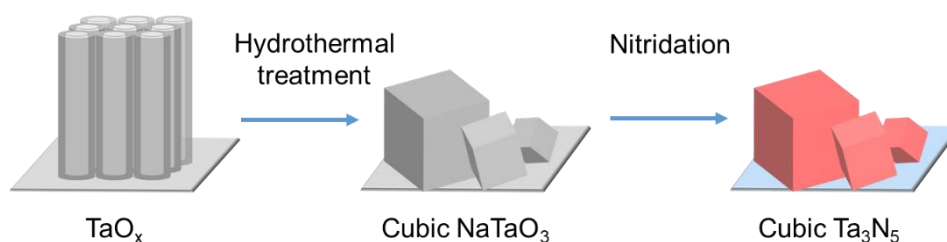
The Ta₃N₅ NTs were synthesized through anodization of Ta foil to form tantalum oxide NTs and subsequent post-annealing in NH₃ to form tantalum nitride according to a modified procedure reported previously.³⁴ For the anodization procedure, tantalum foil (0.127 mm thick, Alfa Aesar) was first cut into pieces 4 cm² in size. Then, one side of the Ta foil was roughened with sandpaper for about 10 min. After the roughening, the Ta foil was cleaned by ultrasonication in acetone, methanol, isopropanol, and deionized (DI) water and dried by flowing air. The electrolyte for anodization was made by mixing 38 mL of sulfuric acid (95–98%, Sigma-Aldrich), 0.4 mL of hydrofluoric acid (48%, Sigma-Aldrich), and 1.6 mL of DI water with vigorous stirring during preparation. The Ta foil was anodized with Pt gauze as the counter electrode at 60 V DC bias for 10 min without stirring. After being thoroughly washed with ethanol and DI water, the as-prepared tantalum oxide NTs were naturally dried in air. The conversion of oxide to nitride was performed in a quartz-tube furnace (Lindberg/Blue M). The temperature was raised from room temperature to 1,000 °C at the rate of 10 °C/min and held at 1,000 °C for 2 hr. After that, the furnace was naturally cooled down to room temperature. Throughout the process, 75 sccm anhydrous NH₃ flowed through the quartz tube, and the pressure in the tube remained at 500 Torr. The Ta₃N₅ sample was scratched on the edge to expose the conductive Ta underneath. Tinned Cu wire was secured to the exposed Ta substrate by Ag epoxy (M.G. Chemicals). Non-conductive hysol epoxy (Loctite 615) was used to seal the sample, except for the exposed area for testing. Typical electrodes were ~0.05 cm² in area.



Scheme 1. Synthesis of Ta₃N₅ NTs

2.2 Preparation of Cubic Ta₃N₅ Photoelectrodes

Tantalum foils (0.127 mm thick, 99.95% purity, Alfa Aesar) were cut into 4 cm² pieces and then one side was sanded with sand paper. By sonicating in acetone, isopropanol, and ethanol, surface impurities were removed. Then it was rinsed with deionized water and dried in air. Porous tantalum oxide films were formed by anodization in a solution of 38 ml sulfuric acid (95–98%, Sigma-Aldrich), 0.4 mL of hydrofluoric acid (48%, Sigma-Aldrich), and 1.6 mL of DI water at 60 V DC for 10 min. After anodization, the porous tantalum oxide films were treated with NaOH solution to obtain NaTaO₃ films. Typically, 15 mL of 2 M NaOH solution was transferred into a Teflon-lined stainless-steel autoclave. Porous tantalum oxide films were then immersed into the solution. The autoclave was sealed and maintained at 200 °C for 24 h and allowed to cool down to room temperature naturally. Finally, Ta₃N₅ films were formed by nitriding the as-prepared NaTaO₃ films in a quartz-tube furnace under NH₃ flow at 1,000 °C for 2 h.¹⁷



Scheme 2. Synthesis of cubic Ta₃N₅.

2.3 Synthesis of Ta₃N₅/polymeric g-C₃N₄ Hybrid Photoanode

Bulk C₃N₄ was synthesized through the polymerization of urea (98 %, Sigma-Aldrich).

Typically, 10 g of urea was placed in a quartz-tube furnace. The temperature was increased to 550 °C at the rate of 10 °C/min in a NH₃ atmosphere and held at this temperature for 3 h. After cooling to room temperature, the resulted light yellow bulk C₃N₄ was collected. Then it was dispersed in isopropanol and sonicated for 1 hour to get g-C₃N₄ solution. Ta₃N₅/polymeric g-C₃N₄ photoanode was prepared by electrophoresis method. Ta₃N₅ electrodes were used as working electrode, a Ta foil was used as counter electrode. After immersing the Ta₃N₅ into g-C₃N₄ isopropanol solution, different potential was applied between working and counter electrodes for different time. Then all the electrodes were washed thoroughly with DI water.

2.4 Deposition of Co-Pi, Co(OH)₂, NiFeOOH and CoNiFeOOH co-catalysts.

CoPi catalyst was deposited using photo-assisted electrochemical deposition method. The precursor solutions were made by mixing 0.01M cobalt(II) nitrate hexahydrate (Co(NO₃)₂·6H₂O, ACS reagent, 98% Sigma-Aldrich) in 0.1 M phosphate buffer solution (pH 7) in the volume ratio of 1:1. Then the deposition of CoPi was carried out under the anodic current of 10 μA/cm² for 10 min while stirring. The electrodes were then washed thoroughly with DI water.

Co(OH)(OCH₃) powders were synthesized based on a modified method. 1 mg Co(OH)(OCH₃) powder was added to 10 mL of DI water and ultrasonicated for 30 min. The supernatant was added to a Teflon autoclave with the Ta₃N₅ NTs facing up, after etching in a mixture of HF:HNO₃:H₂O (1:2:7 v/v/v) for 30 s. The container was placed in an oven at 120 °C for 1 hr. After that, the sample was washed gently in DI water and dried in air.

NiFeOOH and CoNiFeOOH catalysts were deposited using cathodic electrodeposition. For NiFeOOH deposition, a 0.09 M solution of nickel(II) nitrate hexahydrate

($\text{Ni}(\text{NO}_3)_2 \cdot 6\text{H}_2\text{O}$, 98% Alfa Aesar) was purged with N_2 for 20 min. Then 0.01 M of iron(II) chloride (FeCl_2 , 98%, Sigma-Aldrich) was added. The deposition was carried out galvanostatically at -0.1 mA/cm^2 for 10 min without stirring. The electrodes were then washed thoroughly with DI water. The deposition of CoNiFeOOH was in the mixture of 16 mmol nickel(II) nitrate hexahydrate, 10 mmol iron(II) chloride (FeCl_2 , 98%, Sigma-Aldrich) and 16 mmol of cobalt(II) nitrate hexahydrate ($\text{Co}(\text{NO}_3)_2 \cdot 6\text{H}_2\text{O}$, ACS reagent, 98% Sigma-Aldrich) under the anodic current of -0.1 mA/cm^2 for 10 min without stirring.

2.5 Deposition of GaN

GaN was deposited on Ta_3N_5 nanotube using the Cambridge nanotech (Savannah 100) plasma enhanced atomic layer deposition (PE-ALD) system based on previous reports. The Ga precursor was tris(dimethylamino)gallium dimer ($\text{Ga}_2(\text{NMe}_2)_6$, 98%, Strem Chemicals) and NH_3 or N_2 gas was used as plasma and N source. During the deposition, the Ga precursor was heated to $120 \text{ }^\circ\text{C}$ and the growth temperature was varied from 200 and $275 \text{ }^\circ\text{C}$. For each cycle, the pulse time for $\text{Ga}_2(\text{NMe}_2)_6$ was 0.1 s, then purged with N_2 for 10 s, a 40 s pulse for N plasma, a second purge with N_2 for 10 s.

2.6 PEC Measurement

PEC measurement was carried out with a potentiostat (Modulab XM coupled with Modulab XM ECS software) in a three-electrode configuration. The light source was an AM 1.5 solar simulator (100 mW/cm^2 , Solarlight Model 16S-300-M Air Mass Solar Simulator). For water oxidation, the electrolyte was 1 M NaOH (pH 13.6), and the reference electrode was Hg/HgO. For hole scavenger oxidation, the electrolyte was 0.1 M potassium phosphate with 0.1 M $\text{K}_4\text{Fe}(\text{CN})_6$ (pH 10), and the reference electrode was Ag/AgCl. The Ta_3N_5 photoanode served as the working electrode, an Ag/AgCl electrode (for testing electrolytes at pH 10) or an Hg/HgO electrode (for testing

electrolytes at pH 13.6) served as the reference electrode, and a Pt wire served as the counter electrode. The potential was corrected to RHE scale according to the Nernst equation ($E_{\text{RHE}} = E_{\text{Ag/AgCl}} + 0.059\text{pH} + 0.197$ or $E_{\text{RHE}} = E_{\text{Hg/HgO}} + 0.059\text{pH} + 0.098$). Typical linear sweep voltammetry indicated that the potential was swept from negative to positive at a rate of 20 mV/s with stirring. The onset potential is defined as the potential where the logarithm of absolute photocurrent reaches the lowest value in the J-V curves.

2.7 Materials Characterization

Scanning electron microscopy (SEM) (JSM6340F) was used to obtain the perspective and front-view images. The nanotube samples were first scratched from Ta foils and dispersed in isopropyl alcohol by ultrasonication. Then, the dispersion was dropcasted onto a Cu grid for TEM measurement. X-ray diffraction patterns (XRD) was performed on a Bruker D2 PHASER with Cu Ka radiation. Regular XPS measurements were performed with a PHI 5400 XPS system equipped with an Al X-ray source (incident photon energy 1,486.7 eV). The aperture size was set to 1.1 mm in diameter. The binding energy of the obtained XPS spectra was calibrated with respect to the C 1s peak of adventitious carbon at 284.4 eV. Infrared spectrum (IR) was performed with a Thermo Scientific Nicolet Is5 System. Frequencies are reported in wavenumbers (cm^{-1}).

Chapter 3: Data Analysis and Discussion

3.1 Ta₃N₅ NTs/g-C₃N₄ Hybrid Material as Photoanode.

3.1.1 Materials Characterization

We synthesized Ta₃N₅ nanotubes by electrochemical anodization of Ta foil and then performed the NH₃ annealing process. The crystal structure of the Ta₃N₅ NTs was confirmed by X-ray diffraction patterns. As show in Fig. 3a, XRD patterns of the entire Ta₃N₅ NTs structure show that except for Ta₃N₅, the remaining peaks can be assigned to Ta₂N/Ta₅N₆ phases for all the electrodes. The morphology and microstructures were studied by scanning electron microscopy (SEM). From SEM image, it can be clearly seen that Ta₃N₅ nanotubes were formed. As formed Ta₃N₅ NTs has a length of about 2.5 μm. It was also important to be noticed that the nanotubes were covered by a Ta₃N₅ thin film. After deposition of g-C₃N₄, top-view SEM images suggested that the surface of Ta₃N₅ can be uniformly covered by exfoliated g-C₃N₄ nanosheet (Fig.3d). IR was also carried out to confirm the successful deposition of g-C₃N₄ on Ta₃N₅ NTs (Fig. 3b). Obviously new peaks showed up on Ta₃N₅ after deposition of g-C₃N₄. The peak positions also matched well with bare g-C₃N₄ which indicated that electrophoresis method worked well on depositing g-C₃N₄ onto surface of Ta₃N₅.

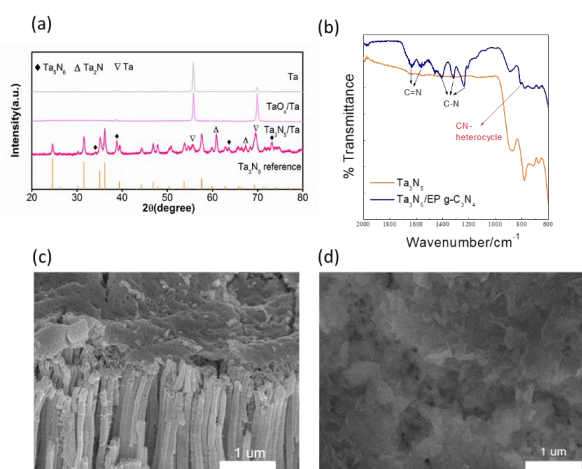


Figure 3. XRD spectrum of bare Ta₃N₅ (a). IR spectrum of Ta₃N₅ and Ta₃N₅/g-C₃N₄ hybrid material (b). SEM images of bare Ta₃N₅ (c) and Ta₃N₅/g-C₃N₄ hybrid material (d).

3.1.2 PEC Performance of Ta₃N₅ NTs/g-C₃N₄ Hybrid Material

As shown in Fig 4a, the performance of all electrodes are almost the same. Since Ta₃N₅ was severely suffered from self-oxidation, the effect of g-C₃N₄ may be hindered by this side reaction. In order to establish the difference more clearly, we conducted PEC characterization with hole scavengers, which are expected to be effective in extracting holes from the photoelectrode under PEC conditions but do not involve O as a necessary intermediate or product. To our surprise, the performance of Ta₃N₅/g-C₃N₄ hybrid material becomes even worse in hole scavenger solution (Fig. 4b). The non-change or even worse performance of the hybrid material could be caused by the poor conductivity of g-C₃N₄.³⁵ Under illumination, the photo-generated holes from Ta₃N₅ would inject into g-C₃N₄, however, due to the poor conductivity of g-C₃N₄, holes can't transfer to water molecules and might recombine inside the g-C₃N₄. Since photo-generated holes were blocked by the protection layer, surface Ta₃N₅ will be self-oxidized to form TaO_x and the performance was dramatically suppressed.

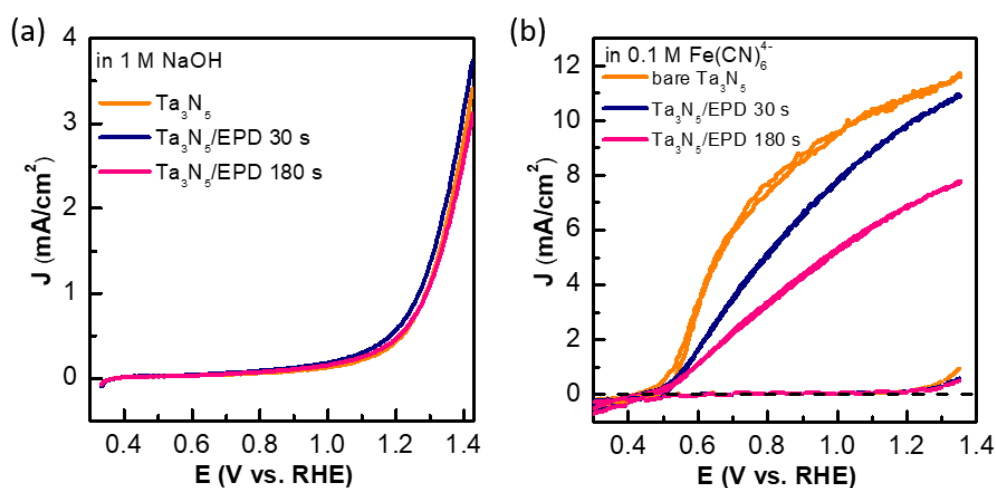


Figure 4. PEC measurement of Ta₃N₅/g-C₃N₄ hybrid photoanode in 1 M NaOH (a) and hole scavenger (b).

As long as the holes cannot be extracted from g-C₃N₄ to H₂O, surface oxidation and recombination will become dominant. Based on previous studies, addition of co-catalysts may help improving the charge transfer between semiconductor and water molecules. In order to improve the poor kinetics between the g-C₃N₄ and water,

different water oxidation catalysts (WOCs) have been used in this work including NiFeOOH, CoPi, Co(OH)₂ and carbon quantum dots.²⁶ Fig. 5 showed the performance of hybrid electrodes with NiFeOOH as co-catalyst. Different deposition time and deposition voltage of g-C₃N₄ was applied to the electrodes for comparison. Changing the time showed that 40 s offered the highest photocurrent. Varying the voltage showed that 60 V gave the best current density, however when the voltage was increased to 80 V, the stability was slightly enhanced with 5 cycles (Table 1). Thus lower voltage may be better. Even though the photocurrent was increased after addition of NiFeOOH, the stability of the hybrid material was not improved. Long-term stability still remained as a problem.

Table. 1 PEC performance of Ta₃N₅/g-C₃N₄/NiFeOOH with different g-C₃N₄ deposition voltage.

Samples	w/o C ₃ N ₄	60 V	80 V	100 V	120 V	140 V
		40 s	40 s	40 s	40 s	40 s
Stability (current remained after 5 cycles at 1.23 V v RHE)	50%	74%	83%	79%	71%	72%
J _{ph} (mA/cm ₂) at 1.23 V v RHE (1 st cycle)	3.0	4.9	3.6	3.2	3.8	3.1

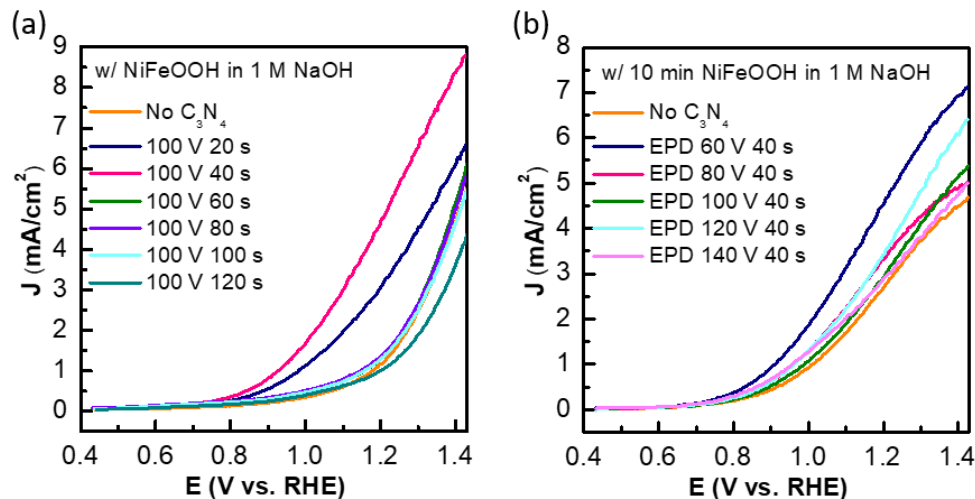


Figure 5. PEC performance of Ta₃N₅/g-C₃N₄ hybrid photoanode with NiFeOOH

(a) Varying the electrophoresis deposition time of g-C₃N₄ while keep voltage at 100V.

(b) Varying the electrophoresis deposition voltage of g-C₃N₄ while keep time for 40 s.

Since NiFeOOH didn't work very well in improving the stability of the hybrid photoelectrodes, other well-known WOCs was also tried. As showed in Fig. 6, after the addition of Co(OH)₂ and CoPi. Photocurrent was not dramatically improved, but the stability was slightly enhanced. However, the improvement was far beyond our expectation.

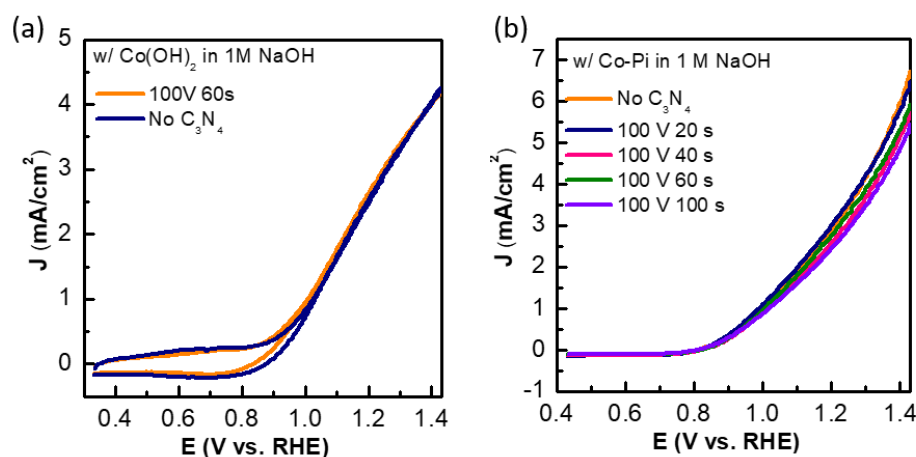


Figure 6. (a) PEC performance of Ta₃N₅/g-C₃N₄ hybrid photoanode with Co(OH)₂. (b) PEC performance of Ta₃N₅/g-C₃N₄ hybrid photoanode with Co-Pi.

Previous research revealed that g-C₃N₄ was not stable under water oxidation conditions, cause H₂O₂, which is a partial oxidation product of water, can attach to g-C₃N₄ strongly.³⁶ The attached H₂O₂ will not only deactivate g-C₃N₄ but may also act as a O source to oxidize Ta₃N₅. Researcher has shown that the existence of carbon nanodots (CDots) (or other H₂O₂ decomposition catalysts such as MnO₂) is critical to the functionality of g-C₃N₄. We plan to use electrochemical synthesis to prepare CDots, which has been previously reported to work well in conjunction with g-C₃N₄. CDOTs was synthesized through a simple electrochemical decomposition of graphite rod and deposited on hybrid electrodes by a simple soaking method.³⁷ Photoluminescence spectra indicated the size of CDots is around 1.5 to 3 nm (Fig.7a).³⁸ From Fig.7, after the introduction of CDots, the stability of Ta₃N₅/g-C₃N₄ was slightly improved but photocurrent was dropped. The improved stability may suggest that addition of CDots helped stabilizing g-C₃N₄, however, this complicated layers may also increase the charge transfer barrier between interfaces which lowered the photocurrent.

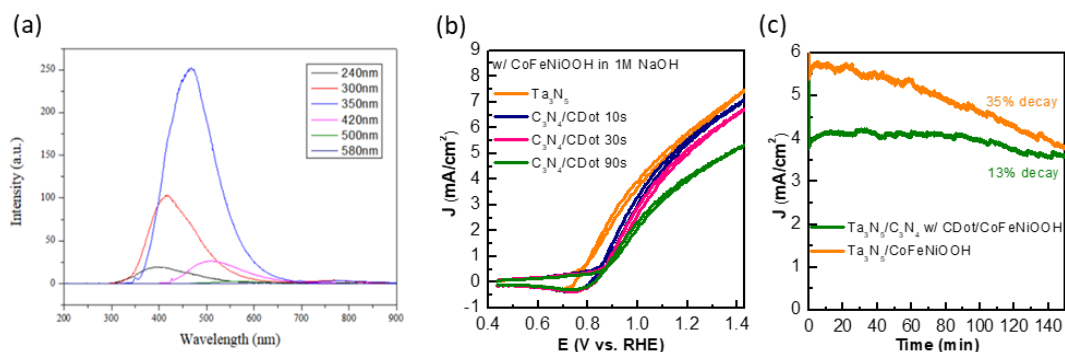


Figure 7. (a) Photoluminescence spectra of CDots. In these figures, the excitation wavelength for the black, red, blue, pink, green and dark blue PL lines are 240, 300, 360, 420, 500, and 580 nm, respectively. (b) PEC measurement of PEC performance of $\text{Ta}_3\text{N}_5/\text{g-C}_3\text{N}_4$ hybrid photoanode with CDots. (c) Stability test of $\text{Ta}_3\text{N}_5/\text{g-C}_3\text{N}_4$ hybrid photoanode with CDots.

3.2 Cubic $\text{Ta}_3\text{N}_5/\text{g-C}_3\text{N}_4$ Hybrid Material as Photoanode.

Even though Ta_3N_5 NTs was considered as a very promising potential photoanode, it may not be the best platform for this study. $\text{g-C}_3\text{N}_4$ was known to have very thin and layered structure, but it may very difficult to have a uniform cover on the top of Ta_3N_5 nanotubes due to its high aspect ratio. Non-uniform cover of $\text{g-C}_3\text{N}_4$ would not act as a protection layer since the exposed Ta_3N_5 could still be oxidized by water. Instead of using nanotube structure, other morphology with smaller aspect ratio should be used. Cubic Ta_3N_5 was successfully synthesized previously and also showed decent performance toward PEC water splitting.

3.2.1 Materials Characterization

Cubic Ta_3N_5 was synthesized by hydrothermal treatment of TaO_x with NaOH and then performed the NH_3 annealing process. The morphology and microstructures were studied by scanning electron microscopy (SEM) and transmission electron microscopy (TEM). Uniform cubic structure can be observed from the SEM images. After deposition of $\text{g-C}_3\text{N}_4$, top-view SEM images and TEM images both suggested that the surface of cubic Ta_3N_5 was uniformly covered by exfoliated $\text{g-C}_3\text{N}_4$ nanosheet (Fig. 8b). IR spectrum was also carried out to confirm the successful deposition of $\text{g-C}_3\text{N}_4$ on cubic Ta_3N_5 (Fig. 8c). New peaks can be clearly observed on Ta_3N_5 after deposition of

g-C₃N₄ which matched well with bare g-C₃N₄.

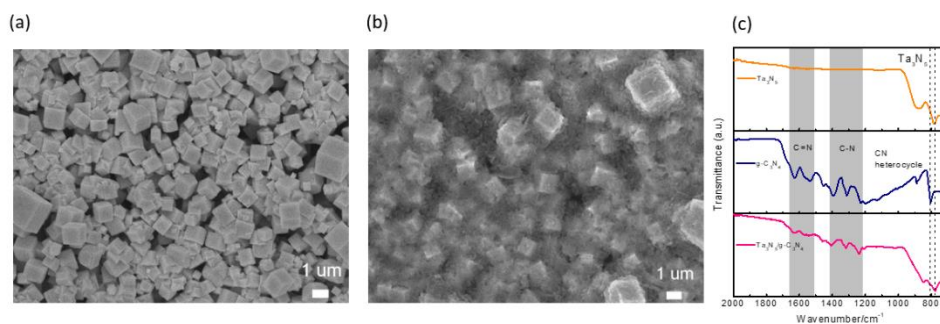


Figure 8. SEM image of bare cubic Ta₃N₅ (a) and cubic Ta₃N₅/g-C₃N₄ hybrid material (b). IR spectrum of Ta₃N₅ and Ta₃N₅/g-C₃N₄ hybrid material (c).

3.2.2 PEC Performance of Cubic Ta₃N₅/g-C₃N₄ Hybrid Material

Based on our findings of applying WOCs on hybrid photoanode, we found NiFe-based catalyst can improve the photocurrent and Co-based catalyst has the ability to make the electrode more stable. Thus, the combination of those two catalysts may offer some synergistic effect and help improving both photocurrent and stability.

After deposition of CoNiFeOOH, samples with g-C₃N₄ showed a higher photocurrent and an earlier turn-on potential. The stability test by potentiostatic measurement suggested that photocurrent of samples with g-C₃N₄ showed less decrease compared with samples without g-C₃N₄ after 1 h illumination.

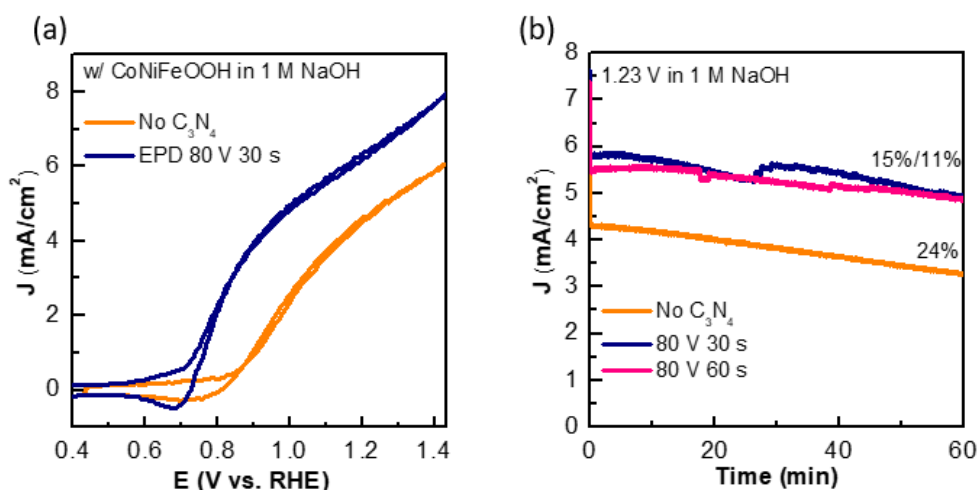


Figure 9. (a) PEC measurement of PEC performance of cubic Ta₃N₅/g-C₃N₄ hybrid photoanode with CoNiFeOOH. (c) Stability test of cubic Ta₃N₅/g-C₃N₄ hybrid photoanode with CoNiFeOOH.

3.3 Ta₃N₅ NTs/GaN as Photoanode.

Among the O free nitrides that could be applied to protect Ta₃N₅, GaN is particularly interesting.³⁹ First, GaN is relatively stable against corrosion compared to other nitrides.⁴⁰⁻⁴² Second, the conduction band of GaN is more negative than those of Ta₃N₅, BaTaO₂N, LaTiO₂N and SrNbO₂N, which tends to mitigate the migration of photogenerated electrons to the GaN on a thermodynamic basis, thus reducing charge recombination.^{14,43} Third, GaN has a long hole lifetime of 10–500 ns that is superior to the lifetimes of (oxy)nitrides, which are generally below 10 ns.^{13,44-45} We assume that by applying GaN on the top Ta₃N₅, the resulting passivated nitride/electrolyte interface can improve stability for solar water splitting.

3.3.1 Materials Characterization

In this work, GaN was first successfully synthesized on SiNWs and fluorinated tin oxide (FTO). SEM images suggested that GaN showed nanowires structures with around 2 μm length. XRD spectrum showed that at 33 and 36 degree two new peaks can be observed compared with bare FTO sample.⁴⁶ This indicates that the surface of the substrates was covered with GaN. However, the weak intensity also suggested that as-prepared GaN had poor crystallinity. Even after post-annealing treatment, GaN didn't show better crystallinity. High resolution XPS spectrum was also carried out to detect the Ga, N and O species. From Ga 3d spectrum, peak at 21.0 eV indicates the existence of Ga-N bond. Peaks at 399.0 and 395.6 eV in N 1s spectrum belong to N-Ga and Ga Auger peak, respectively.⁴⁷⁻⁴⁸ O 1s spectrum showed one peak at 532.3 eV which belonged to O-Ga bond. All the result suggested that the PE-ALD method can be used to synthesize GaN.

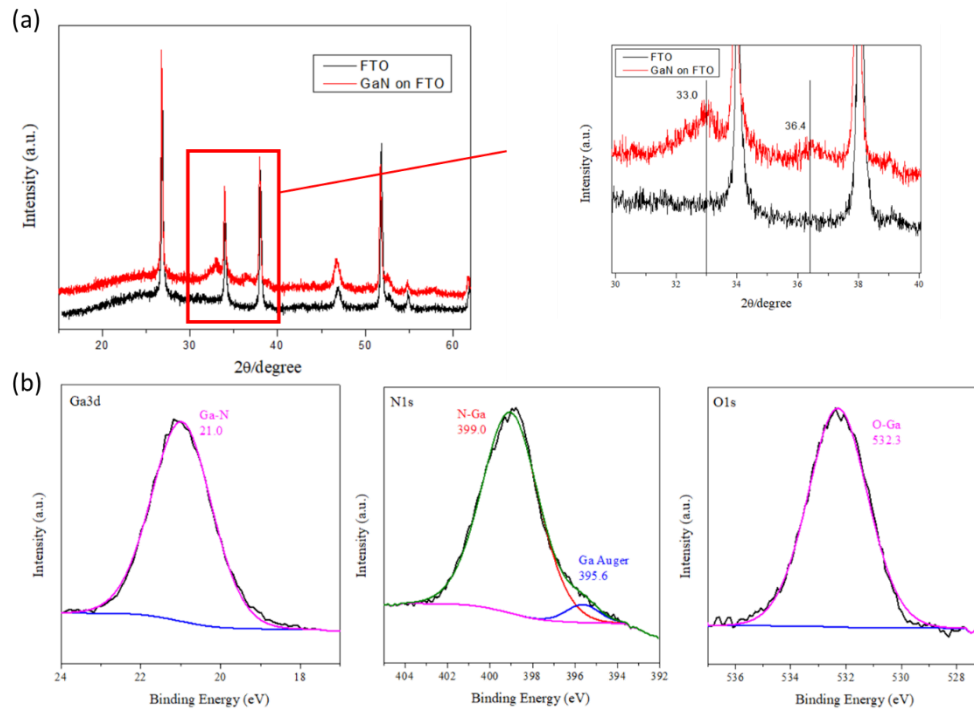


Figure 10. (a) XRD pattern of FTO/GaN. (b) XPS spectrum of FTO/GaN.

Then Ta_3N_5 NTs was used as the substrate and GaN was deposited on the surface by PE-ALD method. SEM images and XPS spectrum of $\text{Ta}_3\text{N}_5/\text{GaN}$ photoanode indicates that GaN was successfully covered the surface of substrate.

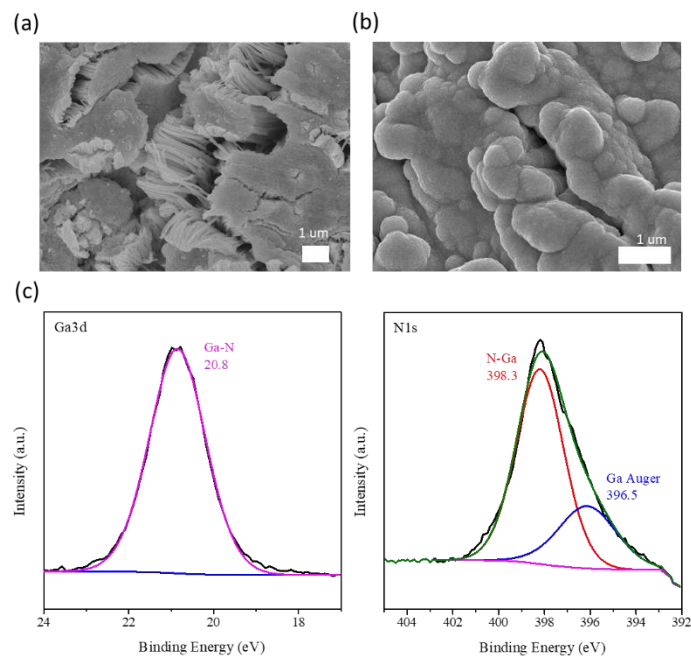


Figure 11. SEM image of bare Ta_3N_5 NTs (a) and $\text{Ta}_3\text{N}_5/\text{GaN}$ (b). XPS spectrum of $\text{Ta}_3\text{N}_5/\text{GaN}$ (c).

3.3.2 PEC Performance of Ta₃N₅/GaN Material

PEC measurement was carried out under normal water splitting conditions using Ta₃N₅/GaN material. NiFeOOH was used as the co-catalysts to enhance the charge transfer between protection layer and H₂O molecules. As show in Fig. , performance of photoanode was decreased after deposition of GaN. The result was out of our expectation. This may be caused by the following reasons. First, Ta₃N₅ was not fully covered by GaN. By using ALD method, we assumed that the surface will be perfectly covered by GaN due to the excellent ability of ALD for coating nanostructures. However, the extremely long length of Ta₃N₅ NTs can result in the failure of uniform cover. Second, as-prepared gallium nitride can only be defined as Ga_xN_y. The exact composition of as-prepared gallium nitride was unrevealed. Without this information, the protection layer may not even be the material we need. Third, the instability of as-prepared gallium nitride. XPS spectrum was carried out after the photoanode was tested under water oxidation conditions (Fig. 12c). Compared with fresh samples, Ga peaks was almost disappeared, but peaks of O-Ta and Ta-O bonds can be clearly observed in O 1s and Ta 4f spectrum.¹⁶ This further suggested that as-prepared gallium nitride was not in its needed form which should be relatively stable under water oxidation conditions. Thus, further optimization of synthesis conditions and more careful characterization are needed to ensure the appropriate GaN is obtained.

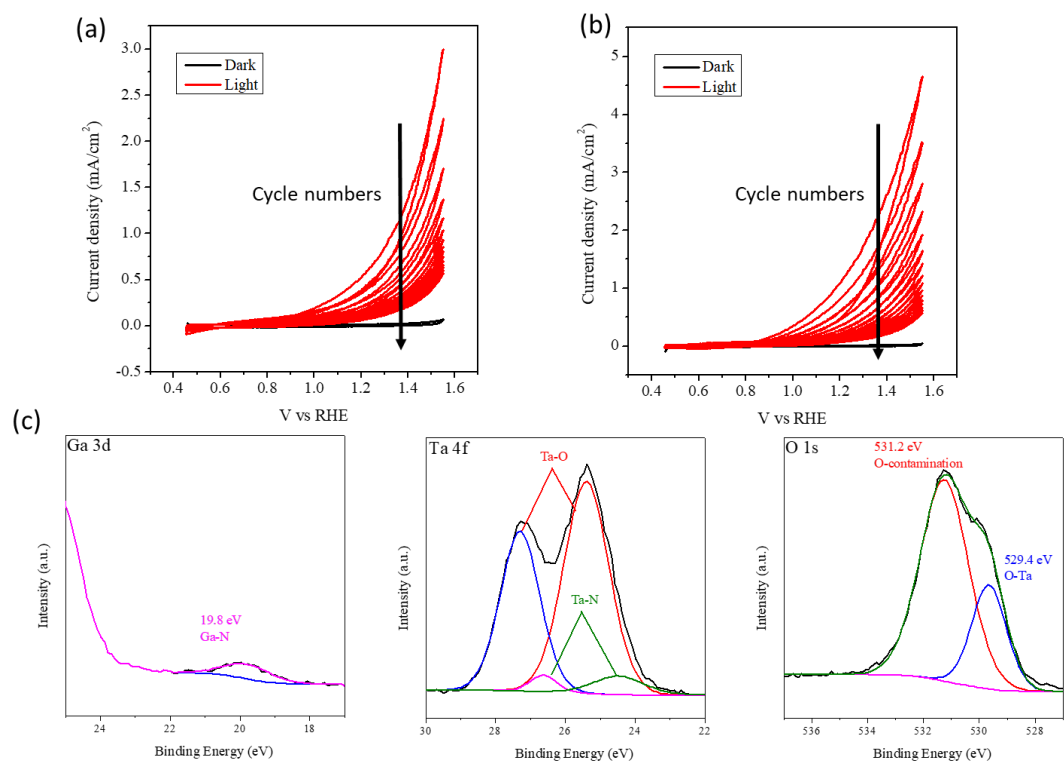


Figure 12. PEC measurement of bare Ta₃N₅ NTs (a) and Ta₃N₅/GaN in 1 M NaOH (b). XPS spectrum of Ta₃N₅/GaN photoanode after PEC test (c).

Chapter 4: Conclusion

Photoelectrochemical (PEC) water splitting on semiconductor electrodes is an efficient method because the energy of sunlight can be directly converted into chemical energy.¹ In this sense, research should be performed for semiconductors with the potentiality to realize high solar-to hydrogen conversion efficiency. However, lots of high performance semiconductors are suffered from instability issue. Among which Ta_3N_5 gained a great interest due to its promising potentials. Previous studies revealed that the instability of Ta_3N_5 is caused by a self-oxidation effect, thus applying an O free protection layer could be a good strategy to solve this problem. In this work, nitride materials like g- C_3N_4 and GaN were used as O free protection layers to enhance the performance of Ta_3N_5 . $\text{Ta}_3\text{N}_5/\text{g-C}_3\text{N}_4$ hybrid materials were successfully synthesized through a simple electrophoresis method. After applying a co-catalyst, the turn-on potential and photocurrent of hybrid photoanodes were both improved. In addition, the stability of the hybrid photoanode was also slightly enhanced. Predictably, an O free protection layer can potentially be an excellent solution to improve the stability of other unstable semiconductors. Further sustained research in mechanisms and applications are necessary for the study in material science and catalysis.

Reference

1. Boddy, P. J., Oxygen Evolution on Semiconducting TiO₂. *J. Electrochem. Soc.* **1968**, *115*, 199-203.
2. Kohl, S.W.; Weiner, L.; Schwartsburd, L.; Konstantinovski, L.; Shimon, L.J.; Ben-David, Y.; Iron, M.A.; Milstein, D., Consecutive thermal H₂ and light-induced O₂ evolution from water promoted by a metal complex. *Science* **2009**, *324* (5923), 74-77.
3. Wang, D.; Sheriff, B. A.; McAlpine, M.; Heath, J. R., Development of ultra-high density silicon nanowire arrays for electronics applications. *Nano. Research* **2008**, *1* (1), 9-21.
4. Lin, Y.; Yuan, G.; Liu, R.; Zhou, S.; Sheehan, S. W.; Wang, D., Semiconductor nanostructure-based photoelectrochemical water splitting: A brief review. *Chem. Phys. Lett.* **2011**, *507* (4-6), 209-215.
5. Fujishima, A.; Honda, K., Electrochemical photolysis of water at a semiconductor electrode. *Nature* **1972**, *238* (5358), 37.
6. Tachibana, Y.; Vayssieres, L.; Durrant, J. R., Artificial photosynthesis for solar water-splitting. *Nat. Photonics* **2012**, *6* (8), 511-518.
7. Luo, J.; Im, J.H.; Mayer, M.T.; Schreier, M.; Nazeeruddin, M.K.; Park, N.G.; Tilley, S.D.; Fan, H.J.; Grätzel, M., Water photolysis at 12.3% efficiency via perovskite photovoltaics and Earth-abundant catalysts. *Science* **2014**, *345* (6204), 1593-1596.
8. Khaselev, O.; Turner, J.A., A monolithic photovoltaic-photoelectrochemical device for hydrogen production via water splitting. *Science* **1998**, *280* (5362), 425-427.
9. Lewis, N. S., Research opportunities to advance solar energy utilization. *Science* **2016**, *351* (6271), aad1920.
10. Zhong, M.; Hisatomi, T.; Sasaki, Y.; Suzuki, S.; Teshima, K.; Nakabayashi, M.; Shibata, N.; Nishiyama, H.; Katayama, M.; Yamada, T.; Domen, K., Highly Active GaN-Stabilized Ta₃N₅ Thin-Film Photoanode for Solar Water Oxidation. *Angew. Chem Int. Ed.* **2017**, *56* (17), 4739-4743.
11. Xie, R.-J.; Bert Hintzen, H. T.; Johnson, D., Optical Properties of (Oxy)Nitride

Materials: A Review. *J. Am. Ceram. Soc.* **2013**, *96* (3), 665-687.

12. Nakamura, R.; Tanaka, T; Nakato, Y., Oxygen Photoevolution on a Tantalum Oxynitride Photocatalyst under Visible-Light Irradiation: How Does Water Photooxidation Proceed on a Metal– Oxynitride Surface? *J. Phys. Chem. B* **2005**, *109* (18), 8920-8927.
13. Ziani, A.; Nurlaela, E.; Dhawale, D. S.; Silva, D. A.; Alarousu, E.; Mohammed, O. F.; Takanabe, K., Carrier dynamics of a visible-light-responsive Ta₃N₅ photoanode for water oxidation. *Phys. Chem. Chem. Phys.* **2015**, *17* (4), 2670-7.
14. Chun, W.J.; Ishikawa, A.; Fujisawa, H.; Takata, T.; Kondo, J.N.; Hara, M.; Kawai, M.; Matsumoto, Y.; Domen, K., Conduction and valence band positions of Ta₂O₅, TaON, and Ta₃N₅ by UPS and electrochemical methods. *J. Phys. Chem. B* **2003**, *107* (8), 1798-1803..
15. Liu, G.; Ye, S.; Yan, P.; Xiong, F.; Fu, P.; Wang, Z.; Chen, Z.; Shi, J.; Li, C., Enabling an integrated tantalum nitride photoanode to approach the theoretical photocurrent limit for solar water splitting. *Energy Environ. Sci.* **2016**, *9* (4), 1327-1334.
16. He, Y.; Thorne, James E.; Wu, Cheng H.; Ma, P.; Du, C.; Dong, Q.; Guo, J.; Wang, D., What Limits the Performance of Ta₃N₅ for Solar Water Splitting? *Chem.* **2016**, *1* (4), 640-655.
17. Liu, G.; Shi, J.; Zhang, F.; Chen, Z.; Han, J.; Ding, C.; Chen, S.; Wang, Z.; Han, H.; Li, C., A tantalum nitride photoanode modified with a hole-storage layer for highly stable solar water splitting. *Angew. Chem. Int. Ed.* **2014**, *53* (28), 7295-9.
18. Ong, W. J.; Tan, L. L.; Ng, Y. H.; Yong, S. T.; Chai, S. P., Graphitic Carbon Nitride (g-C₃N₄)-Based Photocatalysts for Artificial Photosynthesis and Environmental Remediation: Are We a Step Closer To Achieving Sustainability? *Chem. Rev.* **2016**, *116* (12), 7159-329.
19. Sun, M.; Fang, Y.; Kong, Y.; Sun, S.; Yu, Z.; Umar, A., Graphitic carbon nitride (g-C₃N₄) coated titanium oxide nanotube arrays with enhanced photo-electrochemical performance. *Dalton. Trans.* **2016**, *45* (32), 12702-9.
20. Liu, J.; Liu, Y.; Liu, N.; Han, Y.; Zhang, X.; Huang, H.; Lifshitz, Y.; Lee, S.T.;

Zhong, J.; Kang, Z., Metal-free efficient photocatalyst for stable visible water splitting via a two-electron pathway. *Science* **2015**, *347* (6225), 970-974.

21. Nayak, S.; Mohapatra, L.; Parida, K., Visible light-driven novel g-C₃N₄/NiFe-LDH composite photocatalyst with enhanced photocatalytic activity towards water oxidation and reduction reaction. *J. Mater. Chem.* **2015**, *3* (36), 18622-18635.

22. Li, Y.; Wang, R.; Li, H.; Wei, X.; Feng, J.; Liu, K.; Dang, Y.; Zhou, A., Efficient and Stable Photoelectrochemical Seawater Splitting with TiO₂@g-C₃N₄ Nanorod Arrays Decorated by Co-Pi. *J. Phys. Chem. C* **2015**, *119* (35), 20283-20292.

23. Feng, C.; Wang, Z.; Ma, Y.; Zhang, Y.; Wang, L.; Bi, Y., Ultrathin graphitic C₃N₄ nanosheets as highly efficient metal-free cocatalyst for water oxidation. *Appl. Catal. B Environ.* **2017**, *205*, 19-23.

24. Liu, J.; Zhang, Y.; Lu, L.; Wu, G.; Chen, W., Self-regenerated solar-driven photocatalytic water-splitting by urea derived graphitic carbon nitride with platinum nanoparticles. *Chem. Commun. (Camb)* **2012**, *48* (70), 8826-8.

25. Moon, G.-h.; Fujitsuka, M.; Kim, S.; Majima, T.; Wang, X.; Choi, W., Eco-Friendly Photochemical Production of H₂O₂ through O₂ Reduction over Carbon Nitride Frameworks Incorporated with Multiple Heteroelements. *ACS Catal.* **2017**, *7* (4), 2886-2895.

26. Liu, J.; Liu, Y.; Liu, N.; Han, Y.; Zhang, X.; Huang, H.; Lifshitz, Y.; Lee, S.T.; Zhong, J.; Kang, Z., Metal-free efficient photocatalyst for stable visible water splitting via a two-electron pathway. *Science* **2015**, *347* (6225), 970-974.

27. Arrigo, R.; Schuster, M. E.; Abate, S.; Giorgianni, G.; Centi, G.; Perathoner, S.; Wrabetz, S.; Pfeifer, V.; Antonietti, M.; Schlögl, R., Pd Supported on Carbon Nitride Boosts the Direct Hydrogen Peroxide Synthesis. *ACS Catal.* **2016**, *6* (10), 6959-6966.

28. Liu, J.; Liu, N. Y.; Li, H.; Wang, L. P.; Wu, X. Q.; Huang, H.; Liu, Y.; Bao, F.; Lifshitz, Y.; Lee, S. T.; Kang, Z. H., A critical study of the generality of the two step two electron pathway for water splitting by application of a C₃N₄/MnO₂ photocatalyst. *Nanoscale* **2016**, *8* (23), 11956-61.

29. Li, Y.; Zhang, L.; Torres-Pardo, A.; Gonzalez-Calbet, J. M.; Ma, Y.; Oleynikov, P;

- Terasaki, O.; Asahina, S.; Shima, M.; Cha, D.; Zhao, L.; Takanabe, K.; Kubota, J.; Domen, K., Cobalt phosphate-modified barium-doped tantalum nitride nanorod photoanode with 1.5% solar energy conversion efficiency. *Nat. Commun* **2013**, *4*, 2566.
30. Higashi, M.; Domen, K.; Abe, R., Fabrication of efficient TaON and Ta₃N₅ photoanodes for water splitting under visible light irradiation. *Energy & Environmental Science* **2011**, *4* (10).
31. Li, Y.; Takata, T.; Cha, D.; Takanabe, K.; Minegishi, T.; Kubota, J.; Domen, K., Vertically aligned Ta₃N₅ nanorod arrays for solar-driven photoelectrochemical water splitting. *Adv. Mater.* **2013**, *25* (1), 125-31.
32. Seo, J.; Takata, T.; Nakabayashi, M.; Hisatomi, T.; Shibata, N.; Minegishi, T.; Domen, K., Mg-Zr Cosubstituted Ta₃N₅ Photoanode for Lower-Onset-Potential Solar-Driven Photoelectrochemical Water Splitting. *J. Am. Chem. Soc.* **2015**, *137* (40), 12780-3.
33. Lin, Y.; Battaglia, C.; Boccard, M.; Hettick, M.; Yu, Z.; Ballif, C.; Ager, J. W.; Javey, A., Amorphous Si thin film based photocathodes with high photovoltage for efficient hydrogen production. *Nano. Lett.* **2013**, *13* (11), 5615-8.
34. Burke, M. S.; Enman, L. J.; Batchellor, A. S.; Zou, S.; Boettcher, S. W., Oxygen Evolution Reaction Electrocatalysis on Transition Metal Oxides and (Oxy)hydroxides: Activity Trends and Design Principles. *Chem. Mater.* **2015**, *27* (22), 7549-7558.
35. Feng, J.; Liu, G.; Yuan, S.; Ma, Y., Influence of functional groups on water splitting in carbon nanodot and graphitic carbon nitride composites: a theoretical mechanism study. *Phys. Chem. Chem. Phys.* **2017**, *19* (7), 4997-5003.
36. Li, Z.; Kong, C.; Lu, G., Visible Photocatalytic Water Splitting and Photocatalytic Two-Electron Oxygen Formation over Cu- and Fe-Doped g-C₃N₄. *J. Phys. Chem. C* **2015**, *120* (1), 56-63.
37. Xu, Z.; Yu, J.; Liu, G., Fabrication of carbon quantum dots and their application for efficient detecting Ru(bpy)₃²⁺ in the solution. *Sens. Actuator B-Chem.* **2013**, *181*, 209-214.
38. Li, H.; He, X.; Kang, Z.; Huang, H.; Liu, Y.; Liu, J.; Lian, S.; Tsang, C. H.; Yang,

X.; Lee, S. T., Water-soluble fluorescent carbon quantum dots and photocatalyst design. *Angew. Chem. Int. Ed.* **2010**, *49* (26), 4430-4.

39. Kibria, M. G.; Qiao, R.; Yang, W.; Boukahil, I.; Kong, X.; Chowdhury, F. A.; Trudeau, M. L.; Ji, W.; Guo, H.; Himpfel, F. J.; Vayssieres, L.; Mi, Z., Atomic-Scale Origin of Long-Term Stability and High Performance of p-GaN Nanowire Arrays for Photocatalytic Overall Pure Water Splitting. *Adv. Mater.* **2016**, *28* (38), 8388-8397.

40. Zhong, M.; Ma, Y.; Oleynikov, P.; Domen, K.; Delaunay, J.-J., A conductive ZnO–ZnGaON nanowire-array-on-a-film photoanode for stable and efficient sunlight water splitting. *Energy Environ. Sci.* **2014**, *7* (5).

41. AlOtaibi, B.; Harati, M.; Fan, S.; Zhao, S.; Nguyen, H. P.; Kibria, M. G.; Mi, Z., High efficiency photoelectrochemical water splitting and hydrogen generation using GaN nanowire photoelectrode. *Nanotechnology* **2013**, *24* (17), 175401.

42. Hayashi, T.; Deura, M.; Ohkawa, K., High Stability and Efficiency of GaN Photocatalyst for Hydrogen Generation from Water. *Jpn. J. Appl. Phys.* **2012**, *51*.

43. Stevanović, V.; Lany, S.; Ginley, D.S.; Tumas, W.; Zunger, A., Assessing capability of semiconductors to split water using ionization potentials and electron affinities only. *Phys. Chem. Chem. Phys.* **2014**, *16* (8), 3706-3714.

44. Kumakura, K.; Makimoto, T.; Kobayashi, N.; Hashizume, T.; Fukui, T.; Hasegawa, H., Minority carrier diffusion length in GaN: Dislocation density and doping concentration dependence. *Appl. Phys. Lett.* **2005**, *86* (5).

45. Mickevičius, J.; Tamulaitis, G.; Shur, M. S.; Fareed, Q.; Zhang, J. P.; Gaska, R., Saturated gain in GaN epilayers studied by variable stripe length technique. *J. Appl. Phys.* **2006**, *99* (10).

46. Ozgit-Akgun, C.; Goldenberg, E.; Okyay, A. K.; Biyikli, N., Hollow cathode plasma-assisted atomic layer deposition of crystalline AlN, GaN and Al_xGa_{1-x}N thin films at low temperatures. *J. Mater. Chem. C* **2014**, *2* (12), 2123-2136.

47. Kumar, M.; Kumar, A.; Thapa, S. B.; Christiansen, S.; Singh, R., XPS study of triangular GaN nano/micro-needles grown by MOCVD technique. *Mater. Sci. Eng. C* **2014**, *186*, 89-93.

48. Alevli, M.; Gungor, N.; Haider, A.; Kizir, S.; Leghari, S. A.; Biyikli, N., Substrate temperature influence on the properties of GaN thin films grown by hollow-cathode plasma-assisted atomic layer deposition. *J. Vac. Sci. Technol.* **2016**, *34* (1).